Nanoscale Research Letters

NANO EXPRESS Open Access

Investigation of direct inkjet-printed versus spin-coated ZrO_2 for sputter IGZO thin film transistor

Wei Cai[1], Honglong Ning[1*], Zhennan Zhu[1], Jinglin Wei[1], Shangxiong Zhou[1], Rihui Yao[1*], Zhiqiang Fang[2], Xiuqi Huang[3], Xubing Lu[4] and Junbiao Peng[1]

Abstract

In this work, a low leakage current ZrO_2 was fabricated for sputter indium gallium zinc oxide (IGZO) thin-film transistor using direct inkjet-printing technology. Spin-coated and direct inkjet-printed ZrO_2 were prepared to investigate the film formation process and electrical performance for different process. Homogeneous ZrO_2 films were observed through the high-resolution TEM images. The chemical structure of ZrO_2 films were investigated by XPS measurements. The inkjet-printed ZrO_2 layer upon IGZO showed a superior performance on mobility and off state current, but a large V_{th} shift under positive bias stress. As a result, the TFT device based on inkjet-printed ZrO_2 exhibited a saturation mobility of 12.4 cm^2/Vs, an I_{on}/I_{off} ratio of 10^6, a turn on voltage of 0 V and a 1.4-V V_{th} shift after 1-h PBS strain. Higher density films with less oxygen vacancy were responsible for low off state current for the printed ZrO_2 device. The mechanism of deteriorated performance on PBS test can be ascribed to the In-rich region formed at the back channel which easily absorbs H_2O and oxygen. The absorbed H_2O and oxygen capture electrons under positive bias stress, serving as acceptors in TFT device. This work demonstrates the film formation process of direct inkjet-printed and spin-coated oxide films and reveals the potential of direct inkjet-printed oxide dielectric in high-performance oxide TFT device.

Keywords: Oxide dielectric, Direct inkjet printing, Interface, Bias stress stability

Background

Metal oxide dielectrics have recently emerged as promising alternatives to SiO_2 and SiN_x in thin-film transistors (TFTs) owing to their superior properties, including high capacitance, low defect states, and large band gap which leads to high mobility and low off current [1–3]. For these reasons, oxide dielectrics fabricated by vacuum process are widely studied in displays, sensor arrays, and driving circuits [4]. Meanwhile, the solution process has also received remarkable attention because of the advantage of low cost for large-scale fabrication including spin coating, inkjet printing, spray coating, and slit coating [5, 6]. Among these, direct inkjet printing is the most promising method which can achieve patterned films without photolithography. However, TFT devices fabricated by the inkjet-printing process exhibit inferior electrical performances compared to the vacuum-processed ones. Direct inkjet-printing metal-oxide films face serious problems: (1) the uncontrollable spreading of oxide precursor on the substrate due to the difference of surface energy of the fluid and substrate and (2) the compatibility of printed oxide dielectrics with semiconductor [7].

The film formation process of solution-processed dielectric film has significant influence on electrical property. The spin-coating method as an established technique is widely used in solution-processed TFT. The leakage current density of spin-coated oxide dielectric is usually lower than 10^{-6} A/cm^2 at 1 MV/cm, and the breakdown electric field is more than 2 MV/cm. Saturation mobility of TFT based on coated oxide dielectric is around 10 cm^2/Vs. However, for printed oxide dielectric, the leakage current density is about two orders of magnitude higher than that for coated oxide film (>10^{-4} A/

* Correspondence: ninghl@scut.edu.cn; yaorihui@scut.edu.cn
[1]Institute of Polymer Optoelectronic Materials and Devices, State Key Laboratory of Luminescent Materials and Devices, South China University of Technology, Guangzhou 510640, China
Full list of author information is available at the end of the article

Springer Open

© The Author(s). 2019 **Open Access** This article is distributed under the terms of the Creative Commons Attribution 4.0 International License (http://creativecommons.org/licenses/by/4.0/), which permits unrestricted use, distribution, and reproduction in any medium, provided you give appropriate credit to the original author(s) and the source, provide a link to the Creative Commons license, and indicate if changes were made.

cm^2 at 1 MV/cm) and saturation mobility is lower than 5 cm^2/Vs. Few reports have made comparison of inkjet-printed dielectric films with spin-coated films especially on the film formation process. Density, surface roughness and homogeneity of dielectric films are the most important factors related to the electrical performance of TFT [8]. Moreover, the interface between gate insulator and semiconductor also plays a key role for the solution process TFT [9]. A comprehensive study on inkjet-printed oxide dielectrics is of great value to better understand this promising technique.

In this paper, we prepared high-quality ZrO_2 films with favorable surface appearance and excellent electrical performance by both coating and printing method and investigated the electrical effect applied in sputtered indium gallium zinc oxide (IGZO) TFT [10, 11]. The film formation process of the spin-coating and direct printing methods is compared. The spin-coating method is dominated by centrifugal force leading to uniform but dispersive distribution of molecules while the inkjet-printing process depends on fluid dynamics. According to XPS and IV test, inkjet-printed ZrO_2 film (double layers) had less oxygen vacancies compared with the spin-coated one. Increasing printed layers of ZrO_2 films can fill the holes and vacancies created by unsteady flow of precursor spreading on the substrate, contributing to less defect and superior uniformity. the direct inkjet-printed ZrO_2 film for sputtered IGZO has lower leakage current density, higher mobility, larger on/off ratio, and larger V_{th} shift under positive bias stress than the spin-coated ZrO_2-TFT. The In-rich region formed at the back channel of inkjet-printed ZrO_2 TFT is responsible for worse stability since water molecules and oxygen in the air can easily be absorbed in under positive bias stress, consuming electrons from the IGZO layer. It reveals that the direct inkjet-printing technique is able to fabricate high-density oxide dielectric but the interface defect should be well controlled to avoid electrical instability.

Methods

Materials

The ZrO_2 solution was synthesized by dissolving 0.6 M $ZrOCl_2 \cdot 8H_2O$ in a 10 ml mixture solvent of 2-methoxyethanol (2MOE) and ethylene glycol with a ratio of 2:3 to attain a certain surface tension of precursor. The solution was stirred at 500 r/min at room temperature for 2 h, followed by aging for at least 1 day. For ozone UV treatment process, a 100-W UV lamp with 250 nm wavelength was used to irradiate the indium tin oxide (ITO) substrate cleaned by isopropyl alcohol and deionized water. Subsequently, ZrO_2 films were formed by spin coating or direct inkjet-printing process. The coating process was carried out with a speed of 5000 rpm for 45 s, while the drop space and nozzle temperature are 30 μm and 30 °C for the printing process. ZrO_2 films were annealed at 350 °C under atmospheric environment for 1 h. 10-nm-thick IGZO was then grown by direct current pulsed sputtering method with a pressure of 1 mTorr (oxygen:argon = 5%) and patterned by shadow mask. IGZO was annealed at 300 °C for 1 h to reduce the defect in the film. The channel width and length were 550 μm and 450 μm; thus, the width/length ratio was 1.22. Finally, Al source/drain electrodes with 150-nm thickness were deposited by direct current sputtering at room temperature.

Instruments

X-ray photoelectron spectroscopy (XPS) measurements were carried out to investigate the chemical structure in oxide semiconductors performed by ESCALAB250Xi (Thermo-Fisher Scientific, Waltham, MA, USA) at a basic pressure of 7.5×10^{-5} mTorr. The cross-sectional transmission electron microscopy (TEM) images were measured by JEM-2100F (JEOL, Akishima, Tokyo, Japan) and the results of electronic differential system (EDS) mapping scan were analyzed by Bruker (Adlershof, Berlin, Germany) to investigate the element distribution. Under the dark condition and air at RT, capacitance–voltage curves were measured by an Agilent 4284A precision LCR Meter (HP, USA). To measure the transfer characteristics of IGZO TFT and leakage current density curves, we used Agilent 4156C precision semiconductor parameter analyzer. Transfer characteristics were measured by a gate voltage sweeping from − 5 to 5 V with a drain voltage of 5 V. We calculated the field effect mobility using the measured transfer curve and the following equation:

$$I_{DS} = \frac{W\mu C_i}{2L}(V_{GS} - V_{th})^2 \quad (1)$$

where I_{DS}, C_i, μ, W, L, V_{GS}, and V_{th} are the drain current, capacitance of the gate dielectric per unit area, saturation mobility, channel width, channel length, gate voltage, and threshold voltage, respectively. The dielectric constant is calculated by equation as follow:

$$\varepsilon_r = \frac{C \cdot d}{\varepsilon_0 \cdot S} \quad (2)$$

where ε_r, C, d, ε_0, and S are relative dielectric constant, capacitance of the gate dielectric, thickness of the gate dielectric, vacuum dielectric constant, and the area of electrode, respectively.

Result and Discussion

The film formation process of the direct inkjet-printing method compared with the spin-coating method is

proposed in Fig. 1. During the spin coating process, droplets are forced to spread uniformly on the whole substrate by centrifugal force [12]. As a consequence, after the annealing process ZrO_2 molecules are well distributed on the substrate. Meanwhile, the majority of ZrO_2 molecules are tossed out during the coating process, vacancies occur inside the film. The density of films fabricated by spin coating process are irrelevant to coating parameters for certain precursor [13]. For the inkjet-printing process, the printer moves in a particular direction to leave droplets on the substrate. Droplets merge together at the balance of spreading and shrinking process which is influenced by gravity, surface tension and viscoelasticity of precursor. The film formation process of inkjet printing can be well controlled by optimizing processing parameters of droplet space, jet velocity, ink composition, and substrate temperature [14]. The most important factor is drop space set by the printer and post-treatment process for the substrate. Additional file 1: Figure S1 shows images of the contact angle of printing precursor on ITO substrate with different UV treatment periods and the polarizing microscope of annealed ZrO_2 films. ZrO_2 film printed on ITO substrate with 40-s ozone irradiation possesses best morphology. In addition, multiple-layer printing method is efficient in reducing holes in the film by filling vacancies with additional droplets directly printed on the top of the former layer, leading to a more homogeneous film with higher density and less defect [15]. The thickness of films printed 1-layer and 2-layer film is 45 nm and 60 nm, respectively (Additional file 1: Figure S2). Film thickness is not in proportion to printed layers, which explains that the multiple-printing method is not just a thickness accumulation process [16]. In general, the quality of direct-printed ZrO_2 films can be well controlled by processing parameters. In our experiment, we prepare spin-coated (SC), direct inkjet-printed 1-layer (DP1) and 2-layer (DP2) ZrO_2 films and IGZO-TFT devices based on these films to investigate the difference in film morphology and electrical property from different film formation processes.

Figure 2a–c shows the O1s spectrum of ZrO_2 film prepared by different methods. We fitted the oxygen 1s peak to a superposition of three peak components. The peaks centered at 529.8 ± 0.2 eV, 531.7 ± 0.2 eV, and 532.1 ± 0.1 eV can be assigned to metal-oxygen bond species ($V_{M\text{-}O}$), oxygen vacancies (V_O), and weakly bound species ($V_{M\text{-}OR}$), respectively [17, 18]. The $V_{M\text{-}O}$ species of the DP2-ZrO_2 film is 81.57%, which is much higher than the SC-ZrO_2 and DP1-ZrO_2. The V_O species is also the lowest for DP2-ZrO_2 film. This is consistent with ideas mentioned above: (1) direct inkjet-printing process can obtain ZrO_2 film with higher density and less oxygen vacancies, and (2) repeated printing process can fill in the holes and traps and reduce vacancies inside the film. AFM measurement was performed to investigate the surface morphology of printed ZrO_2 film compared with that of spin-coated ZrO_2 shown in Additional file 1: Figure S3. Spin-coated ZrO_2 exhibits the smoothest surface with a surface roughness of 0.29 nm, and direct-printed 1-layer and 2-layer ZrO_2 films are 1.05 nm and 0.67 nm, respectively. Direct-printed ZrO_2 film possesses a rougher surface owing to the uncontrollable flow of fluid during the film formation process [19]. The remarkable decrease in surface roughness from printing one more layer for direct-printed ZrO_2 film can be ascribed to fluid printed on the substrate latter fill up the holes of the initial layer to develop a more homogeneous film. The XPS and AFM results show that the inkjet-printing method has a potential in producing higher quality, lower defect dielectric films compared with spin coating method, along with approximate surface roughness which is suitable for TFT fabrication.

Capacitance-voltage and current-voltage measurements were performed to investigate the electrical properties of SC-ZrO_2 and DP-ZrO_2 film using an Al/ZrO_2/ITO capacitor (metal-insulator-metal) fabricated on glass substrate. We eliminate influence brought by film thickness since they have approximate thickness (60 nm, 45 nm, and 60 nm, respectively). As shown in Fig. 3, DP1-ZrO_2 film exhibits hardly any insulating property, caused by a large number of vacancies in the film which

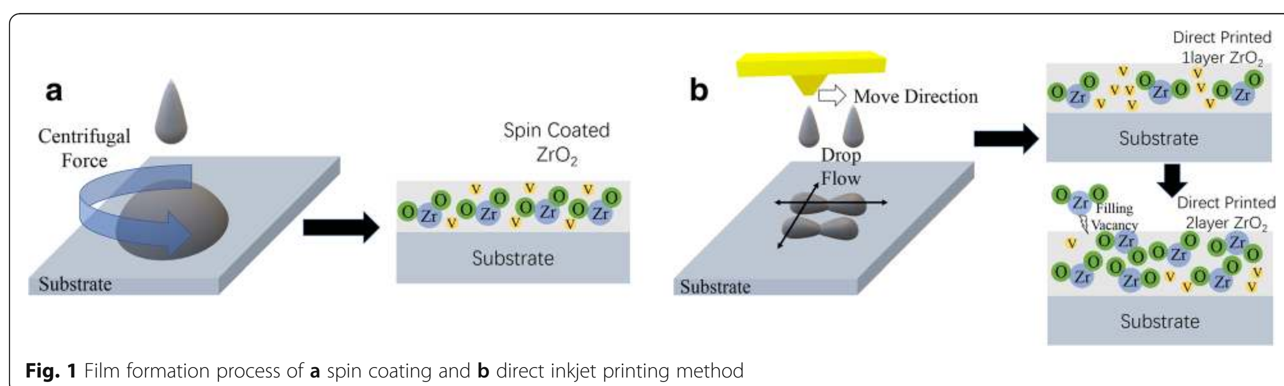

Fig. 1 Film formation process of **a** spin coating and **b** direct inkjet printing method

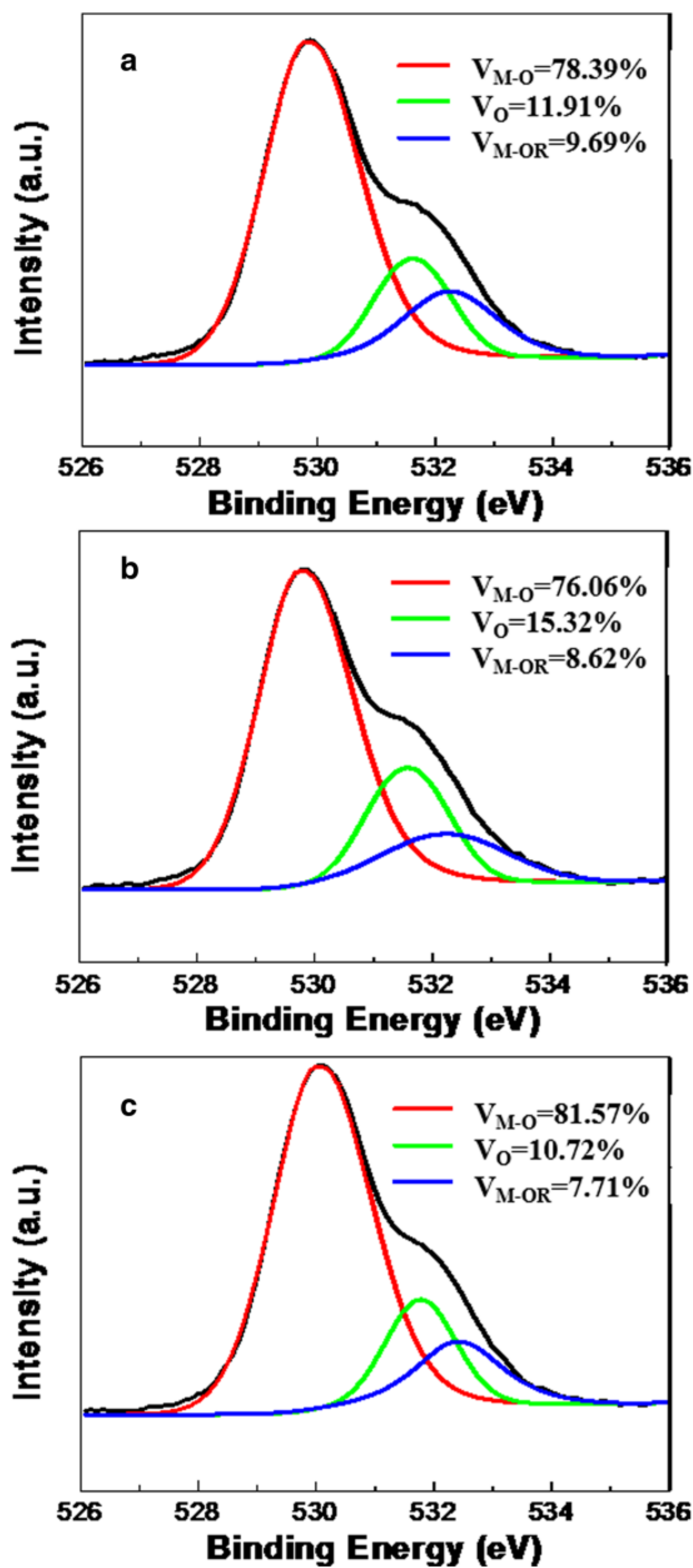

Fig. 2 O1s spectrum of **a** SC, **b** DP1-layer, and **c** DP2-layer ZrO_2 film

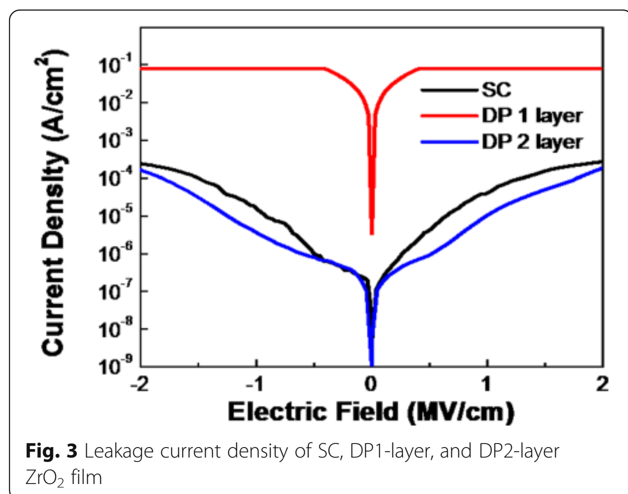

Fig. 3 Leakage current density of SC, DP1-layer, and DP2-layer ZrO_2 film

serve as passage for leakage current. DP2-ZrO_2 film exhibits the best insulating property, consistent with the result of O 1s spectrum mentioned above. As a result, the leakage current density of DP2-ZrO_2 film is 2.4×10^{-5} A/cm^2 at 1 MV/cm and the breakdown voltage is over 2.5 MV/cm. In our experiment, printed more layers are similar on the surface roughness and show little improvement in leakage current density compared with printed 2-layer ZrO_2 film. On the contrary, printing too many layers can easily push the triple line (line of different phase: gas, liquid, solid) moving outward, inducing the nonuniform distribution of precursor ink. Figure 4 shows capacitance-voltage curve of spin-coated and direct-printed ZrO_2 films. The relative dielectric constant for these three samples is calculated to be 19.2, 20.1, and 18.8 which is close to the reference value (18). For both spin-coated and inkjet-printed ZrO_2 films, capacitance density increases with voltage hysteresis is observed in both three samples, and it is smallest in SC-ZrO_2 sample and largest in DP1-ZrO_2 film. The hysteresis is related to the uniformity and defect state of dielectric film. It confirms that the homogeneity of coating ZrO_2 film is the best and multiple layer can improve the uniformity of direct inkjet-printing films [20, 21].

To further study the effect of ZrO_2 layer fabricated by different ways on TFT performance and gate-bias stability, negative gate-bias stress (NBS) and positive gate-bias stress (PBS) results of IGZO-TFT with both SC-ZrO_2 and DP2-ZrO_2 are presented in Fig. 5. Transfer characteristic curves under NBS and PBS were measured by applying a positive (+ 5 V) or negative (− 5 V) bias for 1 h. The DP2-ZrO_2 IGZO TFT shows better performance at static state with a saturation mobility (μ_{sat}) of 12.5 cm^2/V·s, I_{on}/I_{off} radio of 10^6, and V_{th} of 0 V. The SC-ZrO_2 IGZO TFT exhibits an approximate but lower mobility of 10.2 cm^2/V·s, worse I_{on}/I_{off} radio of 2×10^5, and higher off-state current (I_{off}), mainly due to an increase of channel leakage by larger amount of oxygen vacancies (V_O) in the dielectric film. The V_{th} shift of IGZO TFT with both SC-ZrO_2 and DP2-ZrO_2 under NBS measurements is negligible. The negative V_{th} shift of oxide TFTs under NBS is generally caused by the hole trapping or charge injection since the ionized oxygen vacancies can migrate to the semiconductor/insulator interface under the negative gate bias field. The NBS results indicate that either SC-ZrO_2 or DP2-ZrO_2 film has a favorable contact with IGZO [22, 23]. However, unlike SC-ZrO_2 IGZO TFT which exhibits a V_{th} shift of 0.4 V after applying PBS for 1 h, the DP2-ZrO_2 IGZO TFT shows a severe degeneration of performance and large V_{th} shift of 1.2 V under PBS test. The results of ZrO_2-IGZO TFTs under PBS test are summarized in Table 1. Since the V_{th} shift of oxide TFTs under PBS test is generally caused by the diffusion of absorbed water or oxygen molecules, we can assume that the backchannel of DP2-ZrO_2 IGZO TFT is more sensitive to atmospheric environment under PBS test [24, 25].

To investigate the degeneration and V_{th} shift under PBS test for ZrO_2-IGZO TFT, the cross-sectional transmission electron microscopy (TEM) images and EDS line scan were measured to analyze the element distribution. From the cross-sectional TEM images shown in Fig. 6**a** and **b**, a structure of the Al/IGZO/ZrO_2 investigated in this paper was presented. From the high-resolution TEM images of the channel region for

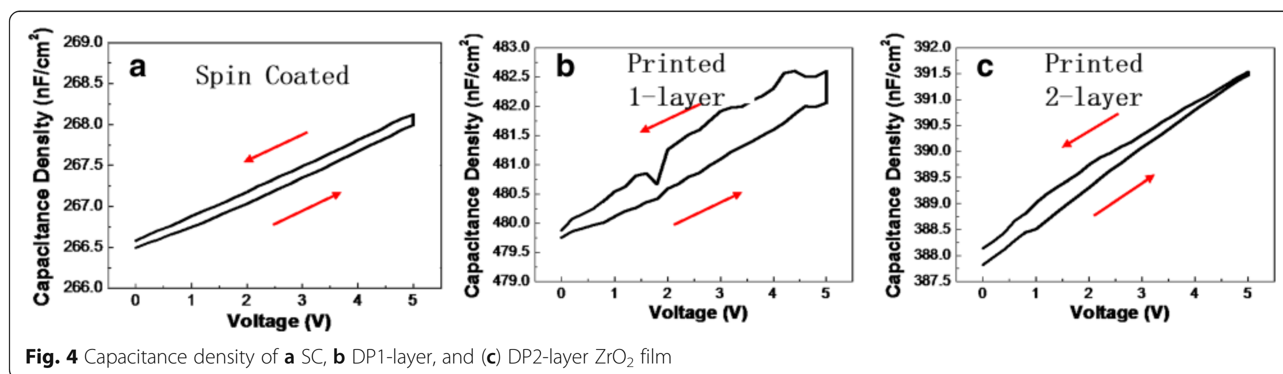

Fig. 4 Capacitance density of **a** SC, **b** DP1-layer, and (**c**) DP2-layer ZrO_2 film

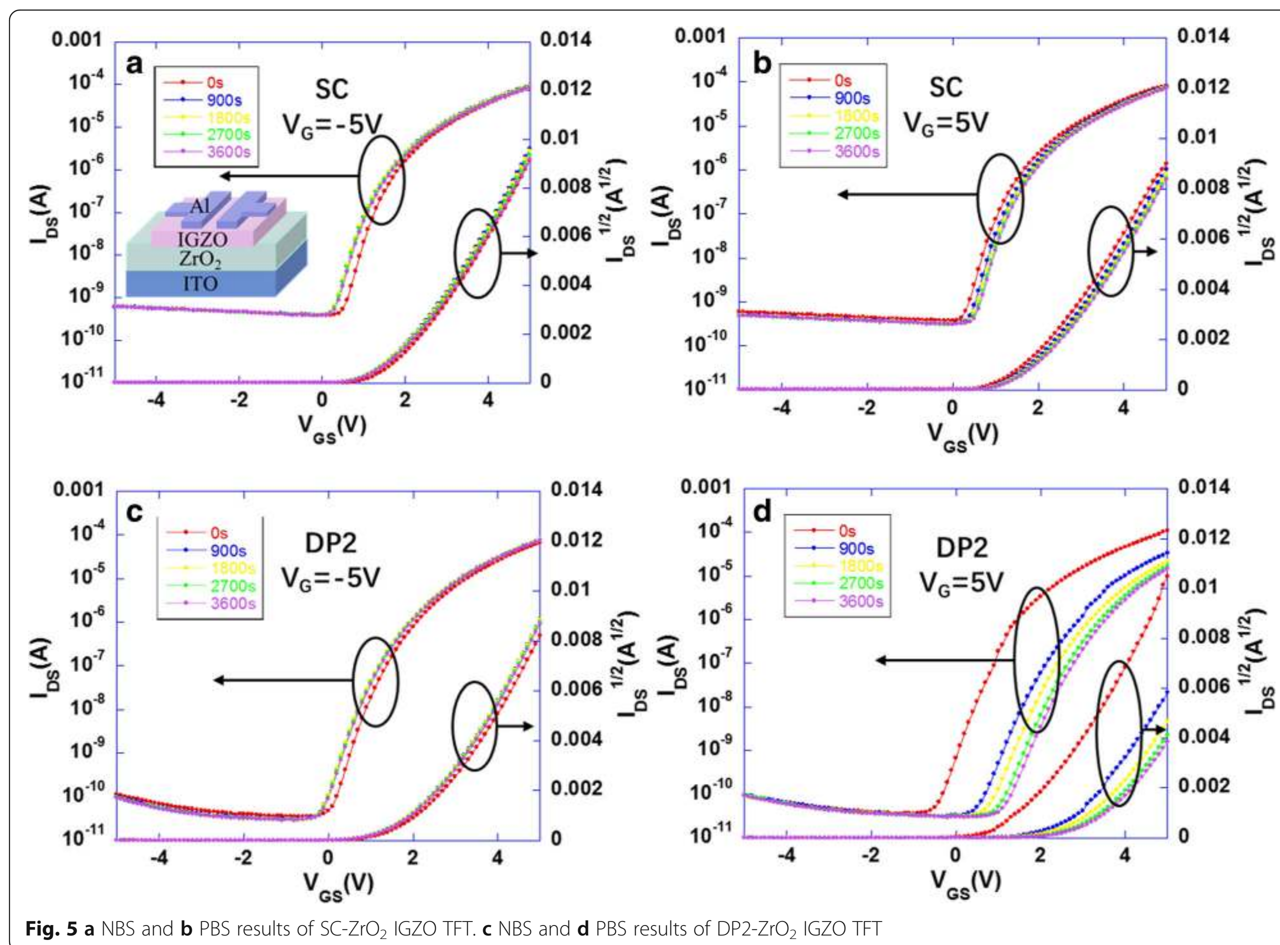

Fig. 5 **a** NBS and **b** PBS results of SC-ZrO_2 IGZO TFT. **c** NBS and **d** PBS results of DP2-ZrO_2 IGZO TFT

Table 1 The summary of mobility, I_{on}/I_{off} ratio, and V_{th} during PBS test of spin-coated and direct-printed ZrO_2 TFT

SC-TFT Time (s)	Mobility (cm^2/V·s)	I_{on}/I_{off} ratio	V_{th} (V)
0	10.2	2.0×10^5	−0.2
900	9.9	1.8×10^5	0.0
1800	9.8	1.7×10^5	0.1
2700	9.6	1.6×10^5	0.1
3600	9.6	1.6×10^5	0.2
DP2-TFT Time (s)	Mobility (cm^2/V·s)	I_{on}/I_{off} ratio	V_{th} (V)
0	12.5	1.0×10^6	−0.6
900	8.8	3.0×10^5	0.3
1800	7.8	1.4×10^5	0.5
2700	7.2	1.0×10^5	0.6
3600	6.8	9.5×10^4	0.7

both SC-ZrO_2 IGZO TFT and DP2-ZrO_2 IGZO TFT, a nearly 8-nm-thick IGZO layer can be obviously observed, which can be proved by the distribution of the In (Ga, Zn) element in EDS line scanning results. Meanwhile, for both SC-ZrO_2 IGZO TFT and DP2-ZrO_2 IGZO TFT, the ZrO_2 layer exhibits an amorphous structure which is beneficial to low-leakage current density. It is obvious that from the line scanning result, Al element diffuse into the IGZO layer, which may be caused by impact during the Al sputtering process. Furthermore, the ratio of Zr and O element is approximately 1:2, which demonstrates that pure ZrO_2 was formed after the annealing process. Uniform distribution of In, Ga, Zn, and Zr elements are also obtained in the IGZO layer for SC-ZrO_2 IGZO TFT, indicating a homogeneous structure of ZrO_2 and IGZO film was established during sputtering and the post-annealing process [19]. But for DP2-ZrO2 IGZO TFT, In, Ga, Zn, O and Zr are in irregular distribution. From Fig. 6(b), we can see the Zr element along with the O element is concentrated at the interface of the dielectric and active layer. And it totally coincided with the analysis of the film formation process of multiple-layer printing method. During the

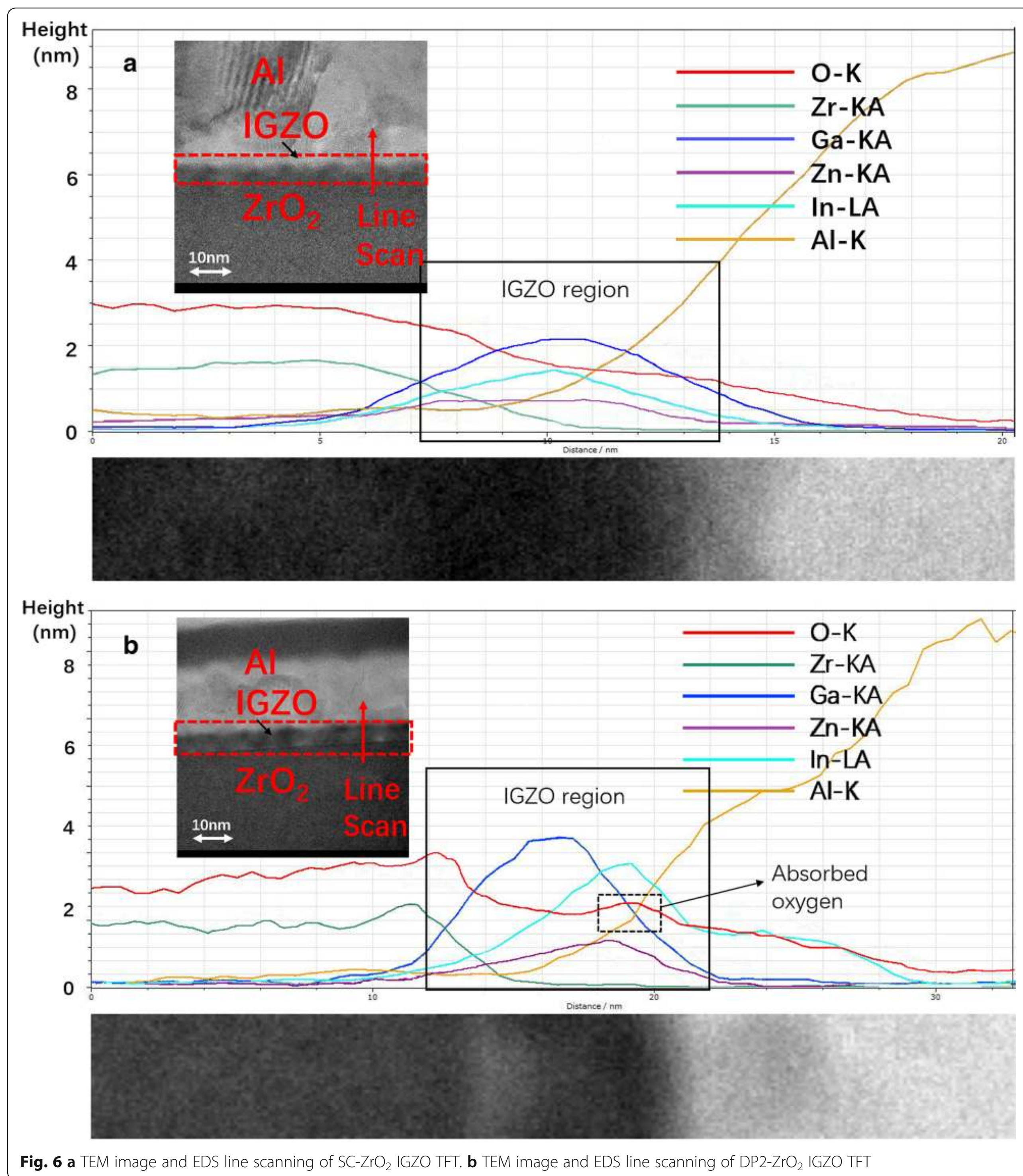

Fig. 6 a TEM image and EDS line scanning of SC-ZrO_2 IGZO TFT. **b** TEM image and EDS line scanning of DP2-ZrO_2 IGZO TFT

multiple-printing process, the precursor printed latter on the substrate partly fills the vacancies, and the majority of droplets are accumulating at the top [26]. Moreover, the segregation of In and Zn element at the backchannel of the IGZO layer is observed in the IGZO layer of printed ZrO_2-TFT. Since the proportion of the Zn element is minimum in our experiment, the electrical performance of IGZO TFT is determined by the In and Ga element. The formation of an In-rich region at the Al/IGZO interface can be concluded as follows: during the annealing process of the IGZO layer which aims to eliminate the defect state of IGZO, there was a

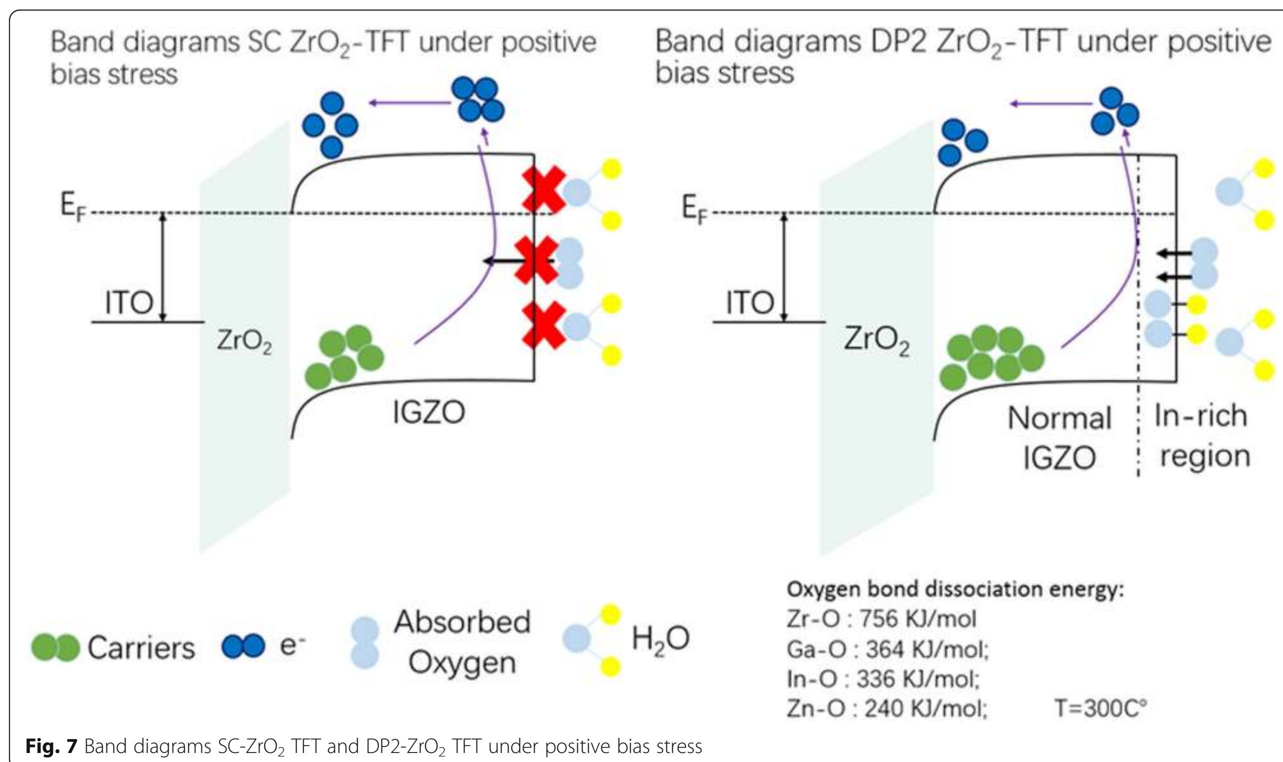

Fig. 7 Band diagrams SC-ZrO_2 TFT and DP2-ZrO_2 TFT under positive bias stress

redistribution of each element. O atoms were "taken away" from In and Zn elements since they have lower oxygen bond dissociation energy than the Zr element, pushing them away from the dielectric/semiconductor interface. The elementary substance of In and Zn elements are unstable so they recombined with oxygen absorbed at the back channel, which can be proved by the EDS scanning [27–29]. The In-rich region with absorbed water molecules and oxygen is the reason for a large V_{th} shift under PBS test.

In order to conceptually depict the mechanism of the degenerated performance and V_{th} shift under positive bias stress for IGZO TFT, schematic band diagrams of TFT for spin-coated ZrO_2 and inkjet-printed ZrO_2 are shown in Fig. 7. DP2-ZrO_2 TFT can accumulate more carriers than SC-ZrO_2 TFT at static state due to a better insulating property, but under positive bias stress, most carriers are exhausted by acceptor-like molecules like water and oxygen in the atmosphere. In general, hydrogen, oxygen, and H_2O molecules will incorporate into the IGZO thin film due to diffusion in the backchannel. Afterwards, the hydrogen will react with oxygen and generate oxygen-hydroxide bonds and consume electrons which results in degenerated performance under positive bias stress. Meanwhile, the adsorbed O_2 and H_2O molecules act as an acceptor-like trap that can capture electrons from conduction band, leading to the positive V_{th} shift after PBS [30]. The degenerated performance and V_{th} shift are unstable and it can recover after hours under an ambient atmosphere. Owing to different oxygen bond dissociation energies of Zr-Oxide (756 kJ/mol), Ga-Oxide (364 kJ/mol), In-Oxide (336 kJ/mol), and Zn-Oxide (240 kJ/mol) [31], O atoms are more likely to combine with the Zr element due to large oxygen bond dissociation energies. The In and Zn element pushed away from ZrO_2/IGZO interface to the backchannel absorb oxygen in the environment. For IGZO TFT using direct inkjet-printed ZrO_2 as gate insulator, large amounts of hydrogen, oxygen, and H_2O molecules "consume" the electrons when applying positive bias stress, leading to degeneration of device performance. Methods including introducing a passivation layer in the top of source/drain electrode for bottom gate structure, using top gate structure, and introducing an interface modification layer between the dielectric and semiconductor layer are effective ways to improve PBS for a solution-processed TFT device, which is interesting and will be carried out in our further research.

Conclusion

In conclusion, we fabricated a high-quality direct inkjet-printed ZrO_2 gate insulator using multiple-layer printing method without extra patterning technology, which is suitable for large-size printing fabrication process. The film formation process demonstrates that ZrO_2 film fabricated by direct inkjet-printing process obtains a denser structure compared with the spin coating process, but the homogeneity is worse because of the

uncontrollable fluid flow of precursor ink. XPS results indicate printed 2-layer ZrO_2 film possesses the highest percentage of M-O-M species ($V_{M\text{-}O}$) and lowest oxygen vacancies (V_O), reflecting in a low leakage current density. Capacitance-voltage curve of DP2-ZrO_2 film shows a slight hysteresis, which is similar with SC-ZrO_2. As a result, DP2-ZrO_2 film exhibits a relatively low leakage current density of 2.4×10^{-5}A/cm^2 at 1 MV/cm and a breakdown voltage over 2 MV/cm; TFT device based on DP2-ZrO_2 exhibited a saturation mobility of 12.4 cm^2/Vs, an I_{on}/I_{off} ratio of 10^6, a turn on voltage of 0 V, and a 1.2-V V_{th} shift after 1 h PBS test. The segregation of the In element at the backchannel of the IGZO layer observed in TEM image and EDS scan can be responsible for larger V_{th} shift during PBS test due to the adsorbed O_2 and H_2O molecules which act as acceptor-like trap that can capture electrons from conduction band. This article presents the advantages of direct inkjet-printing technology and investigates the dielectric property for solution-processed oxide insulator used in oxide TFT device. It demonstrates that DP2-ZrO_2 has a denser structure with less oxygen vacancies, but poor stability under PBS caused by element diffusion. It is promising for direct inkjet-printing technology to be applied in mass production since its low cost and high performance after improving its stability.

Additional file

Additional file 1: Figure S1. Images of contact angle of oxide precursor on ITO substrate for different ozone UV treatment period: (a) 20s, (b) 40s, and (c) 60s and polarizing microscope of annealed ZrO_2 film on ITO substrate for different UV treatment period (d) 20s, (e) 40s, and (f) 60s, respetively. Figure S2. Step profiler images of direct-printed (a) 1-layer and (b) 2-layer ZrO_2 films. Figure S3. AFM images of ZrO_2 film prepared by (a) spin coating, (b)direct-printed 1 layer, and (c) direct-printed 2 layers. (DOCX 2208 kb)

Abbreviations

2MOE: Methoxyethanol (solvent); AFM: Atomic force microscope; Al: Aluminum; DP1/2: Direct-printed 1/2 layer; EDS: Electronic differential system; H_2O: Water molecule; IGZO: Indium gallium zinc oxide (oxide semiconductor); ITO: Indium tin oxide (electrode); O 1s: Oxide 1s atomic orbital; O_2: Oxygen molecule; PBS/NBS: Positive/negative bias stress (test mode); SC: Spin coated; SiN_x: Silicon nitride (dielectric); SiO_2: Silicon Dioxide (dielectric); TEM: Transmission electron microscope; TFT: Thin-film transistor; UV: Ultraviolet; $V_{M\text{-}O}$: Percentage of metal-oxide bond; $V_{M\text{-}OR}$: Percentage of metal-organics bond; V_O: Percentage of oxide vacancy bond; V_{th}: Threshold voltage; XPS: X-ray photoelectron spectroscopy; ZrO_2: Zirconia (oxide dielectric); $ZrOCl_2 \cdot 8H_2O$: Zirconium oxychloride octahydrate (material)

Acknowledgements

This work was supported by National Key R&D Program of China (No.2016YFB0401504), National Natural Science Foundation of China (Grant.51771074, 51521002 and U1601651), National Key Basic Research and Development Program of China (973 program, Grant No.2015CB655004) Founded by MOST, Guangdong Natural Science Foundation (No.2016A030313459 and 2017A030310028), Guangdong Science and Technology Project (No.2016B090907001, 2016A040403037, 2016B090906002 and 2017A050503002), Guangzhou Science and Technology Project (201804020033), the Project for Guangdong Province Universities and Colleges Pearl River Scholar Funded Scheme (2016).

Funding

This work was supported by the Guangdong Science and Technology Project (No.2016B090907001).

Availability of data and materials

Supporting Information is available from Nanoscale Research Letters or from the author.

Authors' contributions

WC, HN, and RY designed the research. WC, ZZ, JW, and SZ carried out the experiments. WC, HN, and RY analyzed the data. ZF, XH, JP, and XL provided valuable discussions and suggestions. WC, HN, and RY wrote the paper. WC, HN, RY, XH, and XL are responsible for this research work. All authors read and approved the final manuscript.

Competing interests

The authors declare that they have no competing interests.

Publisher's Note

Springer Nature remains neutral with regard to jurisdictional claims in published maps and institutional affiliations.

Author details

[1]Institute of Polymer Optoelectronic Materials and Devices, State Key Laboratory of Luminescent Materials and Devices, South China University of Technology, Guangzhou 510640, China. [2]State Key Laboratory of Pulp and Paper Engineering, South China University of Technology, Guangzhou 510640, China. [3]Gu'an New Industry Demonstration Zone, Langfang 065500, Hebei, People's Republic of China. [4]Institute for Advanced Materials and Guangdong Provincial Key Laboratory of Quantum Engineering and Quantum Materials, South China Normal University, Guangzhou 510006, China.

Received: 8 November 2018 Accepted: 18 February 2019
Published online: 05 March 2019

References

1. Fortunato E, Barquinha P, Martins R (2012) Oxide semiconductor thin-film transistors: a review of recent advances. Adv Mater 24:2945–2986
2. Park JS, Maeng W, Kim H, Park J (2012) Review of recent developments in amorphous oxide semiconductor thin-film transistor devices. Thin Solid Films 520:1679–1693
3. Kamiya T, Hosono H (2010) Material characteristics and applications of transparent amorphous oxide semiconductors. Npg Asia Mater 2:15–22
4. Yim K, Yong Y, Lee J, Lee K, Nahm H, Yoo J, Lee C, Seong Hwang C, Han S (2015) Novel high-κ dielectrics for next-generation electronic devices screened by automated ab initio calculations. Npg Asia Mater 7:e190
5. Park S, Kim C, Lee W, Sung S, Yoon M (2017) Sol-gel metal oxide dielectrics for all-solution-processed electronics. Mater Sci Eng R Rep 114:1–22
6. Xu W, Wang H, Ye L, Xu J (2014) The role of solution-processed high-k gate dielectrics in electrical performance of oxide thin-film transistors. J Mater Chem C 2:5389
7. Tong S, Sun J, Yang J (2018) Printed thin-film transistors: research from China. Acs Appl Mater Inter 10:25902–25924
8. Zhu Z, Ning H, Cai W, Wei J, Zhou S, Yao R, X L, Zhang J, Zhou Z, Peng J (2018) Morphology modulation of direct inkjet printing by incorporating polymers and surfactants into a sol-gel ink system. Langmuir 34:6413–6419
9. Ning H, Chen J, Fang Z, Tao R, Cai W, Yao R, Hu S, Zhu Z, Zhou Y, Yang C, Peng J (2017) Direct inkjet printing of silver source/drain electrodes on an amorphous InGaZnO layer for thin-film transistors. Materials 10:51
10. Kaloumenos M, Hofmann K, Spiehl D, Hoffmann R, Precht R, Bonrad K (2016) Electrical properties of solution processed multilayer high-k ZrO_2 capacitors in inert atmosphere. Thin Solid Films 600:59–64
11. Park JH, Yoo YB, Lee KH, Jang WS, JY O, Chae SS, Baik HK (2012) Low-temperature, high-performance solution-processed thin-film transistors with peroxo-zirconium oxide dielectric. Acs Appl Mater Inter 5:410–417
12. Mihi A, Ocaña M, Míguez H (2006) Oriented colloidal-crystal thin films by spin-coating microspheres dispersed in volatile media. Adv Mater 18:2244–2249
13. Yuan Y, Giri G, Ayzner AL, Zoombelt AP, Mannsfeld SCB, Chen J, Nordlund D, Toney MF, Huang J, Bao Z (2014) Ultra-high mobility transparent organic

thin film transistors grown by an off-centre spin-coating method. Nat Commun 5:3005
14. Stringer J, Derby B (2010) Formation and stability of linesproduced by inkjet printing. Langmuir 26:10365–10372
15. Tekin E, Smith PJ, Schubert US (2008) Inkjet printing as a deposition and patterning tool for polymers and inorganic particles. Soft Matter 4:703
16. Jang J, Kitsomboonloha R, Swisher SL, Park ES, Kang H, Subramanian V (2013) Transparent high-performance thin film transistors from solution-processed SnO_2/ZrO_2 gel-like precursors. Adv Mater 25:1042–1047
17. Mi Y, Wang J, Yang Z, Wang Z, Wang H, Yang S (2014) A simple one-step solution deposition process for constructing high-performance amorphous zirconium oxide thin film. RSC Adv 4:6060
18. Son B, Je SY, Kim HJ, Lee C, Lee C, Hwang AY, Won JY, Song JH, Choi R, Jeong JK (2013) High-performance In-Zn-O thin-film transistors with a soluble processed ZrO_2 gate insulator. Phys Status Solidi (RRL) Rapid Res Lett 7:485–488
19. Lee C, Dodabalapur A (2012) Solution-processed high-k dielectric ZrO_2 and integration in thin-film transistors. J Electron Mater 41:895–898
20. Fumagalli L, Ferrari G, Sampietro M, Gomila G (2007) Dielectric-constant measurement of thin insulating films at low frequency by nanoscale capacitance microscopy. Appl Phys Lett 91:243110
21. Liu Y, Guan P, Zhang B, Falk ML, Katz HE (2013) Ion dependence of gate dielectric behavior of alkali metal ion-incorporated aluminas in oxide field-effect transistors. Chem Mater 25:3788–3796
22. Zeumault A, Subramanian V (2016) Mobility enhancement in solution-processed transparent conductive oxide TFTs due to electron donation from traps in high-k gate delectrics. Adv Funct Mater 26:955–963
23. Ji KH, Kim J, Jung HY, Park SY, Choi R, Mo YG, Jeong JK (2011) Comprehensive studies of the degradation mechanism in amorphous InGaZnO transistors by the negative bias illumination stress. Microelectron Eng 88:1412–1416
24. Suresh A, Muth JF (2008) Bias stress stability of indium gallium zinc oxide channel based transparent thin film transistors. Appl Phys Lett 92:33502
25. Liu A, Liu GX, Zhu HH, Xu F, Fortunato E, Martins R, Shan FK (2014) Fully solution-processed low-voltage aqueous In_2O_3 thin-film transistors using an ultrathin ZrOx dielectric. Acs Appl Mater Inter 6:17364–17369
26. Tang W, Zhao J, Huang Y, Ding L, Li Q, Li J, You P, Yan F, Guo X (2017) Bias stress stability improvement in solution-processed low-voltage organic field-effect transistors using relaxor ferroelectric polymer gate dielectric. IEEE Electr Device L 38:748–751
27. Park WJ, Shin HS, Ahn BD, Kim GH, Lee SM, Kim KH, Kim HJ (2008) Investigation on doping dependency of solution-processed Ga-doped ZnO thin film transistor. Appl Phys Lett 93:83508
28. Kwon JM, Jung J, Rim YS, Kim DL, Kim HJ (2014) Improvement in negative bias stress stability of solution-processed amorphous In-Ga-Zn-O thin-film transistors using hydrogen peroxide. Acs Appl Mater Inter 6:3371–3377
29. Kim Y, Han J, Park SK (2012) Effect of zinc/tin composition ratio on the operational stability of solution-processed zinc-tin-oxide thin-film transistors. IEEE Electr Device L 33:50–52
30. Huh J, Jeon J, Choe H, Lee K, Seo J, Ryu M, Park SK, Hwang C, Cheong W (2011) Effects of the composition of sputtering target on the stability of InGaZnO thin film transistor. Thin Solid Films 519:6868–6871
31. Bell RC, Zemski KA, Justes DR, Castleman AW (2001) Formation, structure and bond dissociation thresholds of gas-phase vanadium oxide cluster ions. J Chem Phys 114:798

Submit your manuscript to a SpringerOpen journal and benefit from:

- ► Convenient online submission
- ► Rigorous peer review
- ► Open access: articles freely available online
- ► High visibility within the field
- ► Retaining the copyright to your article

Submit your next manuscript at ► springeropen.com